Multiplet effects in the electronic structure of heavy rare-earth metals

Multiplet effects in the electronic structure of heavy rare-earth metals

S Lebègue[1,2]**, A Svane**[3]**, M I Katsnelson**[4]**, A I Lichtenstein**[5] **and O Eriksson**[1]

[1] Department of Physics, University of Uppsala, SE-75121 Uppsala, Sweden
[2] Laboratoire de Cristallographie et de Modélisation des Matériaux Minéraux et Biologiques, UMR 7036, CNRS-Université Henri Poincaré, BP 239, F-54506 Vandoeuvre-lès-Nancy, France
[3] Department of Physics and Astronomy, University of Aarhus, DK-8000 Aarhus C, Denmark
[4] Institute for Molecules and Materials, Radboud University Nijmegen, NL-6525 ED Nijmegen, The Netherlands
[5] Institute of Theoretical Physics, University of Hamburg, 20355 Hamburg, Germany

Abstract
The spectroscopic properties of elemental terbium, dysprosium, holmium, and erbium are investigated using first-principles calculations taking into account intra-atomic correlation effects. In order to describe the strongly localized f electrons together with the conduction bands, we have used the multiband Hubbard-I approximation to reproduce the multiplet features present in the experimental spectra. A comparison with available experimental data is made and the overall agreement is found to be good.

(Some figures in this article are in colour only in the electronic version)

1. Introduction

Due to the rarity of their natural occurrence in our everyday life, materials containing elements where the electron states partially fill the f shell are often viewed as somewhat exotic. The first series in the Periodic Table with f electrons is in fact called the rare-earth series. Nevertheless, materials containing f elements have found several important applications, e.g. as vital components of permanent magnets in start engines in cars [1], in nuclear technology [2], as giant magnetostrictive materials, in optical fibres [3], and even in smoke detectors in our homes. Among many other things, terbium (Tb) is used in the production of electronic devices, dysprosium (Dy) for compact discs, holmium (Ho) to generate strong magnetic fields, and erbium (Er) as a photographic filter.

The complexity of these elements originates from the mixture of strongly localized (and correlated) f electrons together with the more delocalized spd electrons. Experimentally one of the best ways to study this behaviour is via photoelectron spectroscopy, and this has been

done numerous times [4]. The measured spectra reveal both distinct peaks related to atomic-like multiplets, and broader features related to dispersive bands. The theoretical description of photoemission in f materials is challenging, due to the rather different behaviour of the electrons that need to be incorporated, together with the lattice periodicity. Concerning the heavier lanthanides and their compounds, their spectral properties have usually been analysed using atomic multiplet theory [5–8] or the single-impurity Anderson model [9–12]. However these models rely on a number of adjustable parameters, and for example do not take into account the wavevector dependence of the problem. Also, the density functional theory (DFT) [13, 14] in the local density approximation (LDA) has been applied to these systems, but failed to simulate the whole spectrum [15], although total energy calculations based on DFT have successfully calculated the trivalent ground state and equilibrium volume of the rare-earth elemental solid [16, 17]. Therefore, these works can only be considered as intermediate steps towards a more complete understanding. Considering the potential applications of rare earths in materials science, as well as the fundamental theoretical challenge, efforts have to be pursued towards more predictive and reliable theories.

A tool of choice for computing the excited state properties of strongly correlated systems is the Hubbard-I approximation [18], including both the full atomic part of the problem and the lattice periodicity in a unified framework. The purpose of the present work is to apply this technique to study the photoemission of the heavy lanthanides Tb, Dy, Ho, and Er. The paper is organized as follows: in section 2 we quickly review the Hubbard-I method that we use, in section 3 we present our results and discuss them in comparison with experimental data; finally, in section 4, we offer our conclusions and perspectives of our work.

2. The Hubbard-I approximation

As stated in the introduction, we use the Hubbard-I approximation (HIA) [18] to compute the spectral function of the lanthanide elements. We have to resort to such a method since more traditional electronic structure methods based on DFT are unable to reproduce multiplets in the spectrum, which are often observed in strongly correlated systems [19]. This method has already been applied successfully to samarium [20] and thulium [21] compounds. Here we give a brief review of the method; a more complete description may be found in [19].

The first step is to solve by exact diagonalization the following Hubbard Hamiltonian for an atomic f^n shell:

$$H^{at} = \frac{1}{2} \sum_{\{m_j\}} U_{m_1 m_2 m_3 m_4} c_{m_1}^\dagger c_{m_2}^\dagger c_{m_3} c_{m_4} + \xi \sum_i \vec{l}_i \cdot \vec{s}_i - \mu \sum_m c_m^+ c_m \qquad (1)$$

in order to obtain eigenvalues E_γ and eigenvectors $|\gamma\rangle$ (the index m_j label the f orbitals, running from 1 to 14). Notice that the spin–orbit interaction is included in the model since it cannot be ignored for f electrons. Also, μ is the chemical potential treated as an adjustable parameter in order to embed the atom in the solid. The $U_{m_1 m_2 m_3 m_4}$ are the four-centre integrals written as usual as a product of Gaunt coefficients times the Slater integrals F^ℓ [19].
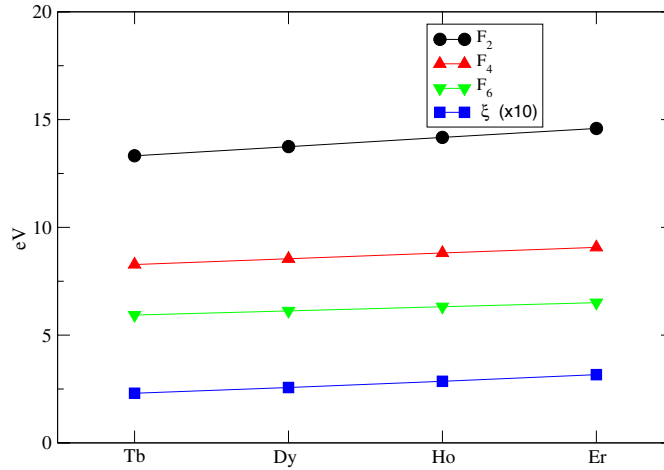
The second step is to calculate the atomic Green function $G_{mm'}^{at}$

$$G_{mm'}^{at}(\omega) = \frac{1}{Z} \sum_{\gamma\delta} \frac{\langle \gamma | c_m | \delta \rangle \langle \delta | c_{m'}^\dagger | \gamma \rangle}{\omega + E_\gamma - E_\delta} (e^{-\beta E_\gamma} + e^{-\beta E_\delta})$$

and the atomic self-energy

$$\Sigma_{mm'}^{at}(\omega) = \omega \delta_{mm'} - (G^{at})_{mm'}^{-1}(\omega) \qquad (2)$$

from the eigenvectors and eigenvalues of H^{at}. Here, β denotes the inverse of the temperature and Z the partition function.

Figure 1. Calculated Slater integrals (in eV) together with the spin–orbit constant ξ (in eV, and scaled up by a factor 10 on this plot) used in the Hubbard-I calculations.

Finally, the atomic self-energy and the Hamiltonian from an LDA calculation are combined in order to get the final Green function $G_{\mathbf{k}}$:

$$G_{\mathbf{k}}^{-1}(\omega) = \omega - \Sigma^{\text{at}}(\omega) - H_{\mathbf{k}}^{\text{LDA}}. \tag{3}$$

By this procedure, we have a Green function that contains both the strong correlation effects and the kinetic energy, with a k dependence, which is mandatory for a problem with periodicity. To be compared with experimental photoemission spectra, the Green function is integrated over the Brillouin zone to get the spectral function $A(\omega)$:

$$A(\omega) = \frac{1}{\pi} \operatorname{Im} \sum_{\mathbf{k}} G_{\mathbf{k}}(\omega). \tag{4}$$

In our case, the parameters F^{ℓ} and ξ are calculated from the f partial waves of the self-consistent LDA calculation. However, due to the lack of complete screening in the LDA approximation, the first Slater integral has to be reduced from its bare calculated value. For all the materials studied we have chosen the same value of $F^0 = 7$ eV. A short discussion of the Hubbard-I approximation in comparison with other methods like the LDA$+U$ [22] and the charge transfer multiplet model [23] has been conducted previously (see [21]) and will not be repeated here.

3. Results and discussion

In this section, we use the Hubbard-I formalism presented above to obtain the spectral functions of Tb, Dy, Ho, and Er. These elements all crystallize in the same crystal structure (hexagonal close packed—hcp) [24], with the only difference being the number of f electrons, which increases from 8 for Tb to 11 for Er. Therefore, they offer a unique testing ground for our method, since the analysis of the results will not be affected by effects related to different crystal structures and the hybridization with the spd conduction electrons will be similar for all of them.

As stated previously, the parameters of our model are obtained from *ab initio* calculations and presented in figure 1. The increase of the values along the series reflects the increased Coulomb interaction in the shell. Also, the calculated spin–orbit constant (denoted as ξ in figure 1 and scaled by a factor 10 to make it visible) is very close to the pure atomic values given by [25], reflecting the high degree of localization of the 4f states.
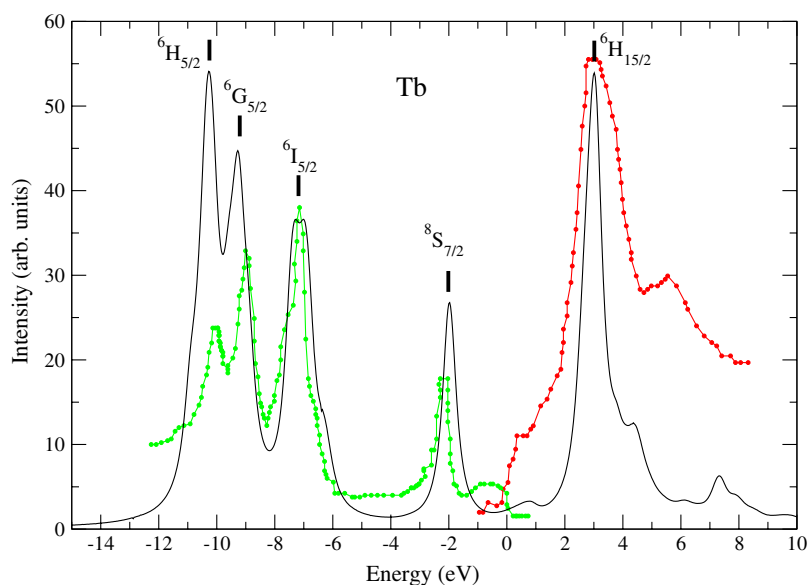
Figure 2. The calculated f contribution to the spectral function of terbium at the equilibrium volume computed within the Hubbard-I method (full line) compared with XPS (green dots) and BIS (red dots) spectra of [4]. The Fermi level is at zero energy.

To start our analysis, the spectral function of terbium is shown in figure 2 and it is compared with the XPS (x-ray photoemission spectroscopy) and BIS (bremsstrahlung isochromat spectroscopy) spectra of [4]. The ground state of Tb corresponds to an f^8 configuration; therefore the XPS (BIS) spectrum is obtained by calculating excitations from f^8 to f^7 (f^8 to f^9). The overall agreement is quite good, all the measured structures being reproduced. For occupied states, the peak at -2.5 eV (corresponding to an f^7 $^8S_{7/2}$ final state with seven spin-parallel electrons) is found to be too low by about 0.2 eV. At larger binding energy the spectrum contains three lines involving an $S = 5/2$ final state. The first of these structures (around -7 eV and corresponding to a ^6I final state) is reproduced very well, while the subsequent peaks, at -9 eV (^6G state) and -10 eV (^6H state), are found at slightly too low energy in comparison with experiments. As regards the unoccupied states, the main peak of the BIS experiment is well placed in energy, about 3 eV above the Fermi level. The second broader structure around 5.5 eV is not reproduced by our f spectral function because the experimental curves show the total observed photoelectron spectrum. To compute the full spectrum one needs to add the f and non-f spectral functions including the appropriate dipole matrix elements with the final state of the photoelectron, which was not attempted here. For the same reason, we do not reproduce the hump between 0 and -1.5 eV. However, these missing features corresponds roughly to the non-f density of states given by the LDA, and therefore are not a limitation of the present theory.

Dysprosium, with an f^9 ground state configuration, is the element following Tb in the Periodic Table. We have used the calculated parameters as presented in figure 1 to produce the spectrum of figure 3 corresponding to transitions to the f^8 multiplet (for states below the Fermi level) and to transitions f^{10} (for states above the Fermi level. The photoemission spectrum is composed of peaks corresponding to ^7F, ^5D, ^5L, ^5K, ^5I multiplets of the f^8 final states. With the Hubbard-I method, we reproduce all the structures, with the ^5D and ^5L being placed at somewhat too low binding energy by approximatively 0.5 eV. The states above the Fermi level
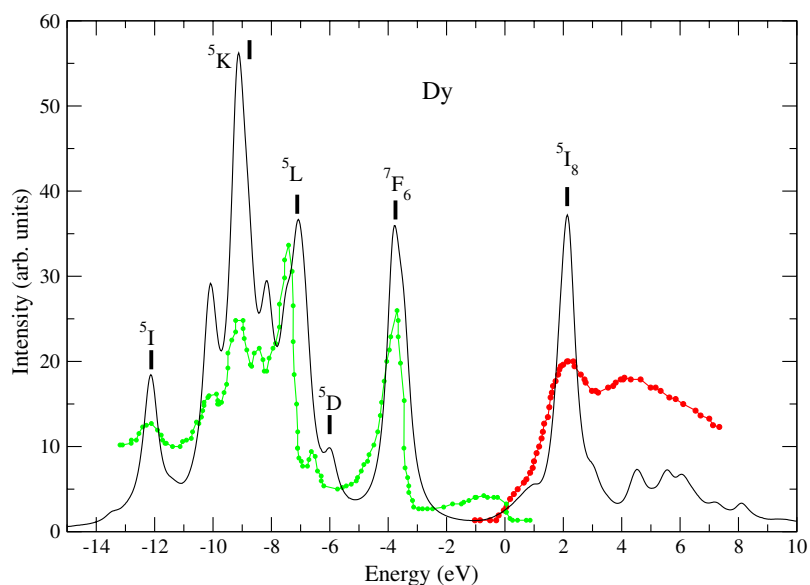
Figure 3. The calculated f contribution to the spectral function of dysprosium at the equilibrium volume computed within the Hubbard-I method (full line) compared with XPS (green dots) and BIS (red dots) spectra of [4]. The Fermi level is at zero energy.

are essentially well reproduced, with the possible deviation at the rather broad experimental feature between 3 and 6 eV, that we find as more detailed, sharp structures between 4.5 and 6 eV. A contribution from non-f electrons is also expected in this range of energy.

Holmium (with 10 electrons in the f shell) is the next element in the series. The lowest transition corresponds to a $^6H_{15/2}$ final state below the Fermi level and to a $^4I_{15/2}$ final state above the Fermi level (see figure 4). As for terbium and dysprosium, we are able to reproduce the experiment of Ho with a very good accuracy. The triple peak between -4 and -6 eV is well reproduced by the theory. The main disagreement is at high binding energy (around -8 eV), where the experiment produce only one peak with a shoulder on the left, whereas our calculations give a double structure. The BIS spectrum is reproduced as well: the main peak at 2 eV and the long tail towards high energy are present.

Finally, as the last element we study erbium. In this case the atomic Hubbard Hamiltonian (equation (1)) is solved for 11 electrons in the shell for the ground state and 10 and 12 electrons for the final states of XPS and BIS, respectively. The quite complicated spectrum with many multiplets is reproduced as shown by figure 5. The first occupied and unoccupied states (corresponding to $^5I_8$ and $^3H_6$ final states) are reproduced correctly with respect to their position in energy. We are even resolving more precisely the structure of the peak at 2 eV in the BIS spectrum since it appears from our calculation to be in fact composed of two spin–orbit split lines. However, the high binding energy structures (occupied states) are shifted in our case by approximatively 1 eV towards larger binding energy in comparison with experiments.

4. Conclusion

The XPS and BIS spectra of Tb, Dy, Ho, and Er have been calculated using the multiband Hubbard-I approximation and compared to available experimental data. The overall agreement
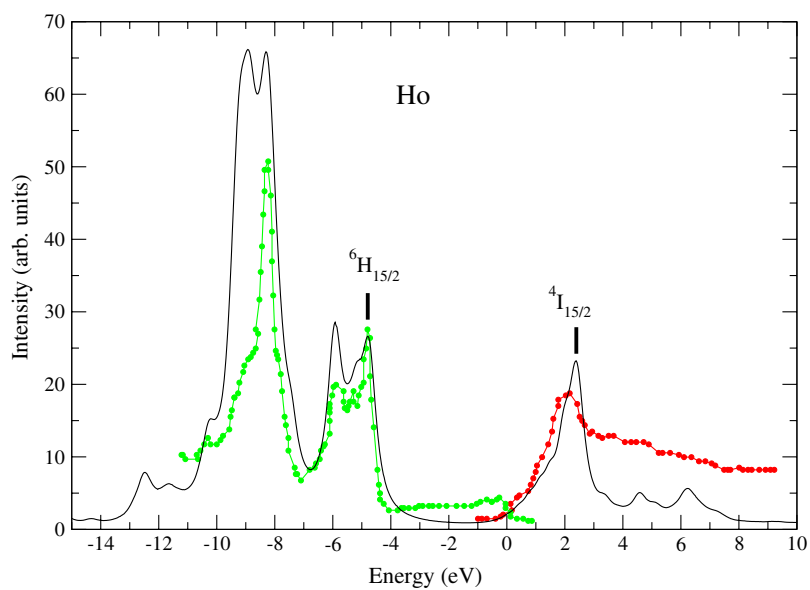
Figure 4. The calculated f contribution to the spectral function of holmium at the equilibrium volume computed within the Hubbard-I method (full line) compared with XPS (green dots) and BIS (red dots) spectra of [4]. The Fermi level is at zero energy.
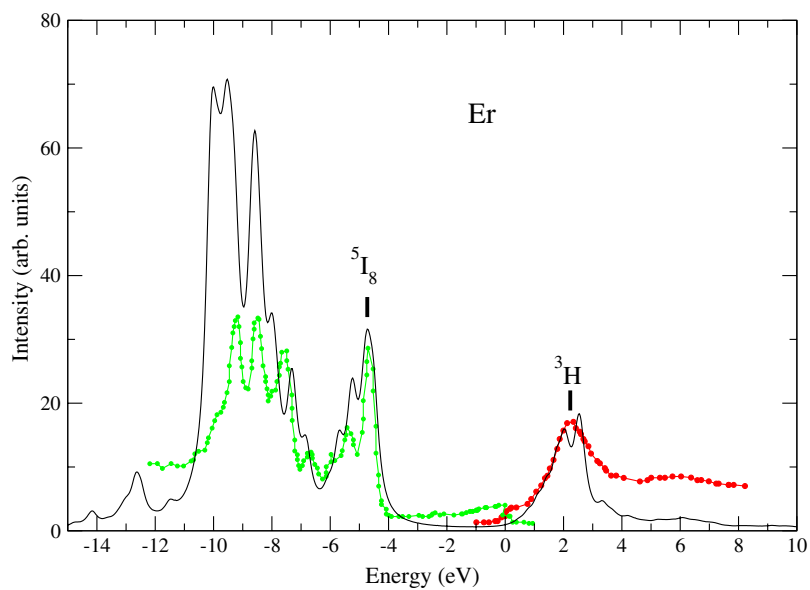
Figure 5. The calculated f contribution to the spectral function of erbium at the equilibrium volume computed within the Hubbard-I method (full line) compared with XPS (green dots) and BIS (red dots) spectra of [4]. The Fermi level is at zero energy.

has been found to be excellent, all the multiplet structures being reproduced successfully. For the four spectral densities of states presented here, a better agreement could probably be achieved by tuning the values of the Slater parameters; however we prefer to keep a scheme

as much *ab initio* as possible in order to have a predictive ability. It is worth noticing that magnetic circular dichroism in photoemission for Tb [7, 8] and Dy have been measured [26]. By averaging over the two polarizations (which correspond roughly to the older experiments of [4]), no additional information can be extracted for comparison with our calculations.

As perspectives to this work, the study of the 4f states of heavy rare earths in intermetallic compounds with the multiband Hubbard-I method should be of high interest since it has been found that the f states in some cases hybridize strongly [12]. Also, the study of the light rare earths within the same framework is interesting and is planned as the next step of the present work.

Acknowledgments

References

[1] Coey J M D (ed) 1996 *Rare-Earth Iron Permanent Magnets* (Oxford: Clarendon)
[2] Manes L (ed) 1985 *Actinides—Chemistry and Physical Properties* (Berlin: Springer)
[3] Desurvire E 1994 *Phys. Today* **1** 20
[4] Lang J K, Baer Y and Cox P A 1981 *J. Phys. F: Met. Phys.* **11** 121
[5] Cox P A, Lang J K and Baer Y 1981 *J. Phys. F: Met. Phys.* **11** 113
[6] Gerken F 1983 *J. Phys. F: Met. Phys.* **13** 703
[7] Starke K, Baumgarten L, Arenholz E, Navas E and Kaindl G 1994 *Phys. Rev.* B **50** 1317
[8] Starke K, Hu Z, Hubinger F, Navas E, Kaindl G and van der Laan G 1999 *Eur. Phys. J.* B **12** 171
[9] Anderson P W 1961 *Phys. Rev.* **124** 41
[10] Tjeng L H *et al* 1993 *Phys. Rev. Lett.* **71** 1419
[11] Weschke E, Grigoriev A Y, Schussler-Langeheine C, Mazumdar C, Meier R, Vandre S, Ram S, Kilian L, Kaindl G and Sutter C 1999 *Phys. Rev. Lett.* **83** 584
[12] Molodtsov S L, Kucherenko Y, Vyalikh D V, Behr G, Starodubov A and Laubschat C 2003 *Phys. Rev.* B **68** 193101
[13] Hohenberg P and Kohn W 1964 *Phys. Rev.* **136** B864
[14] Kohn W and Sham L J 1965 *Phys. Rev.* **140** A1133
[15] Min B I, Jansen H J F, Oguchi T and Freeman A J 1986 *J. Magn. Magn. Mater.* **61** 139
[16] Delin A, Fast L, Johansson B, Wills J M and Eriksson O 1999 *Phys. Rev. Lett.* **79** 4637
[17] Strange P, Svane A, Temmerman W M, Szotek Z and Winter H 1999 *Nature* **399** 756
[18] Hubbard J 1963 *Proc. R. Soc.* A **276** 238
     Hubbard J 1964 *Proc. R. Soc.* A **277** 237
[19] Lichtenstein A I and Katsnelson M I 1998 *Phys. Rev.* B **57** 6884
[20] Svane A, Kanchana V, Vaitheeswaran G, Santi G, Temmerman W M, Szotek Z, Strange P and Petit L 2005 *Phys. Rev.* B **71** 045119
[21] Lebègue S, Santi G, Svane A, Bengone O, Katsnelson M I, Lichtenstein A I and Eriksson O 2005 *Phys. Rev.* B **72** 245102
[22] Anisimov V I, Aryasetiawan F and Lichtenstein A I 1997 *J. Phys.: Condens. Matter* **9** 767
[23] de Groot F 2005 *Coord. Chem. Rev.* **249** 31
[24] *Landolt–Börnstein-Group III Condensed Matter* 1989 (Berlin: Springer)
[25] Gerken F and Schmidt-May J 1983 *J. Phys. F: Met. Phys.* **13** 1571
[26] Arenholz E, Navas E, Starke K, Baumgarten L and Kaindl G 1995 *Phys. Rev.* B **51** 8211